Original Research

Effect of Graphene Nanoplatelets addition on mechanical properties of pure aluminum using a semi-powder method

Muhammad Rashad[a,b,*], Fusheng Pan[a,b,c,*], Aitao Tang[a,b], Muhammad Asif[d]

[a]College of Materials Science and Engineering, Chongqing University, Chongqing 400044, China
[b]National Engineering Research Center for Magnesium Alloys, Chongqing University, Chongqing 400044, China
[c]Chongqing Academy of Science and Technology, Chongqing 401123, China
[d]School of Materials Science and Engineering, Dalian University of Technology, Dalian 116024, China

Abstract

In recent years, graphene has attracted considerable research interest in all fields of science due to its unique properties. Its excellent mechanical properties lead it to be used in nano-composites for strength enhancement. This paper reports an Aluminum–Graphene Nanoplatelets (Al/GNPs) composite using a semi-powder method followed by hot extrusion. The effect of GNP nano-particle integration on tensile, compressive and hardness response of Al is investigated in this paper. It is demonstrated that 0.3 wt% Graphene Nanoplatelets distributed homogeneously in the matrix aluminum act as an effective reinforcing filler to prevent deformation. Compared to monolithic aluminum (in tension), Al–0.3 wt% GNPs composite exhibited higher 0.2% yield strength ($+14.7\%$), ultimate tensile strength ($+11.1\%$) and lower failure strain (-40.6%). Surprisingly, compared to monolithic Al (in compression), Al–0.3 wt% GNPs composite exhibited same 0.2% compressive yield strength and lower ultimate compression strength (-7.8%), and lower failure strain (-20.2%). The Al–0.3 wt% GNPs composite exhibited higher Vickers hardness compared to monolithic aluminum ($+11.8\%$). Scanning electron microscopy (SEM), Energy-Dispersive X-ray Spectroscopy (EDS) and X-ray diffraction (XRD) were used to investigate the surface morphology, elemental percentage composition, and phase analysis, respectively.

1. Introduction

Since the ground-breaking experiment by Andre Geim and Kostya Novoselov [1], graphene has awakened considerable research interest in the field of material science and engineering community. This two-dimensional material, consisting of sp[2]-hybridized carbon atoms, has unique mechanical [2], thermal [3] and electrical properties [4]. It has 1 TPa modulus of elasticity and fracture strength of 125 GPa. One possible way to harnessing the graphene's extraordinary properties for application is to incorporate and disperse graphene in different material matrices i.e. polymers, metals and ceramics. Graphene has widespread applications in the field of electronics and polymer reinforcement. However there are only few reports on metal–graphene composites. In the field of Thermal interface materials (TIMs) graphene (thermally conductive nano-material) has been used as excellent fillers. The strong graphene coupling to metal matrix particles caused an increase in thermal conductivity of resulting composite up to 2300% [5–7].

Aluminum, a low density metal and its alloys have attracted considerable interest in the field of aerospace and automobile industry in order to reduce fuel consumption and emission of

*Corresponding authors at: Chongqing University, College of Materials Science and Engineering, Chongqing 400044, China. Tel.: +86 23 65112635; fax: +86 23 67300077.

E-mail addresses: rashadphy87@gmail.com (M. Rashad), fspan@cqu.edu.cn (F. Pan).

carbon dioxide gas. Metal aluminum has good electrical, thermal and corrosion resistive properties [8,9]. Owing to high ductility, workability and strength to weight ratio, it has widespread applications in vehicles, household appliances containers, etc. [10].

Aluminum based metal matrix composites (MMCs) can be obtained by diffusing reinforcement particles in metal Al using solid or liquid phase methods. Over the past decade, carbon nanotubes (CNTs) have been extensively used as reinforcement of aluminum, to meet high and ever increasing demand of structural strength [11]. Though CNT/Al composites are widely investigated but still uniform dispersion of CNTs is a big challenge for the researchers, which prohibit its use in practical applications. Graphene Nanoplatelets (GNPs) which are two dimensional structures can be dispersed in all kinds of solvents and matrices easily as compared to CNTs. Therefore we are confident to replace the CNT/Al composite by GNP/Al composite in future using different techniques. Powder metallurgy techniques (PM) which consist of basic three steps (mixing, compacting, and sintering) offers homogeneous and uniform distribution of reinforcement particles in the matrix. Our novel nano-processing route is free of ball milling. As ball milling is considered a big problem because it produces heat which can burn powder easily. Therefore our method can be an alternative of ball milling and it has a great potential for synthesis of Al based matrix nano-composite which is considered good for engineering applications.

The objective of this study is to investigate the effects of Graphene Nanoplatelets (GNPs) additives on mechanical properties of Al using the powder metallurgy technique. In earlier work Wang et al. [12] have prepared Al/GNS composite by using 0.3 wt% of Graphene Nano sheets (GNS). They used a complicated experimental procedure and composite prepared had tensile strength of not more than 249 MPa with 0.3 wt% GNS. The objective of this study is to enhance the tensile strength of Al/GNP composite by using the same amount (0.3 wt%) of GNPs by adopting a simple, time saving and efficient method. Mechanical properties of prepared GNP/Al composite are investigated using tensile, compression and hardness tests. Scanning electron microscopy (SEM) and X-ray diffraction are used to examine the micro-structures of the prepared composite.

2. Experimental

2.1. Materials characteristics

Aluminum powder with 99% purity was bought from Shanghai Customs Golden Powder Material Co., Ltd., China. Graphene Nanoplatelets (GNPs) were supplied by Nanjing Xian Feng Nano Material Technology Co., Ltd., Jiangsu, China. Fig. 1 shows the SEM micrographs of as received aluminum powder (a) and Graphene Nanoplatelets (GNPs) (b). An average thickness of Graphene Nanoplatelets (GNPs) was 5–15 nm. Particle size of the as received aluminum was 1–3 µm, and the densities of aluminum powder and Graphene Nanoplatelets (GNPs) were 2.7 g/cm^3 and 2.25 g/cm^3 respectively.
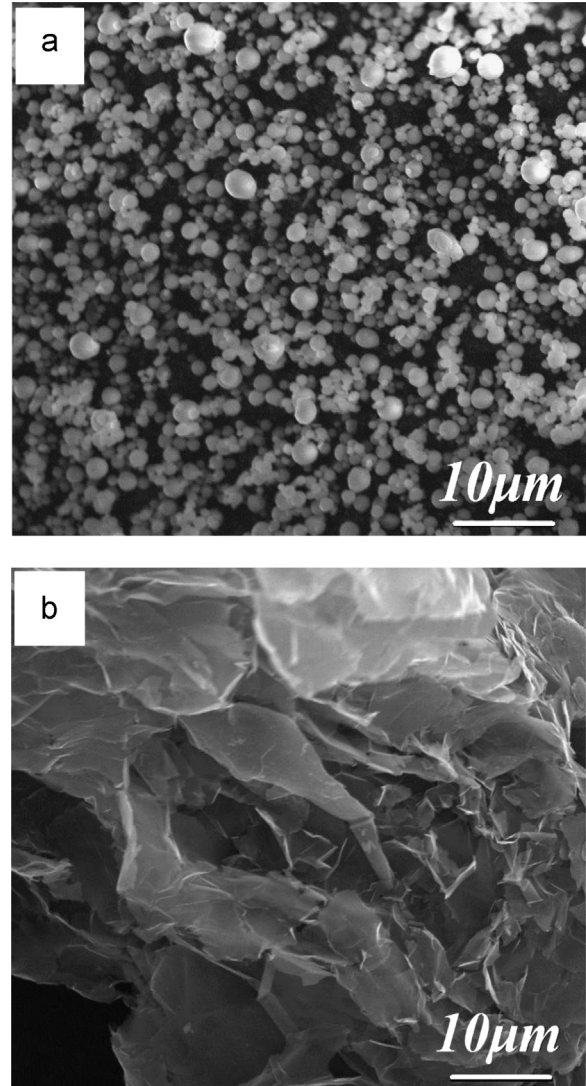

Fig. 1. FESEM image of (a) pure aluminum powder; (b) Graphene Nanoplatelets.

2.2. Synthesis of GNP/Al composite

At first Graphene Nanoplatelets (GNPs) were ultra sonicated in acetone for 1 h. At the same time, aluminum powder was immersed in acetone using mechanical agitator. After ultra-sonication, Graphene Nanoplatelets (GNPs) with particle contents of 0.3 wt% were slowly added to the aluminum powder slurry in acetone. Mixing process was continued for one hour using mechanical agitator to obtain the homogeneity in mixture. The mechanically agitated mixture was filtered and vacuum dried for 12 h at 70 °C to obtain the composite powder. The composite powder was compacted in a stainless steel mold at room temperature under the pressure of 170 MPa to obtain green billet with ⌀30 × 30 mm dimensions. After compacting, the green billets were sintered in muffle furnace at 600 °C for 6 h followed by hot extrusion at 470 °C to obtain the rods of 16 mm diameter. The extrusion ram speed was 1 m/min. For comparison pure Al sample was also prepared using the same method excluding the graphene addition.

Tensile samples with a gauge length of 25 mm and 5 mm diameter and compressive samples with a length of 12 mm and 8 mm diameter were machined from the extruded rods.
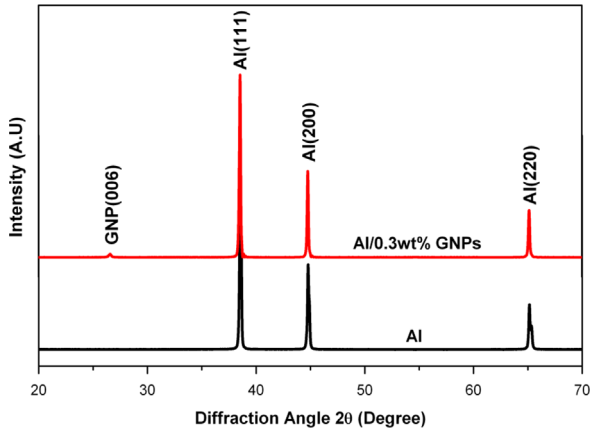

Fig. 2. XRD of pure aluminum and GNP/Al composite.

Mechanical tests were conducted at room temperature with initial strain speed of $1 \times 10^{-3}\,\mathrm{s}^{-1}$ and three samples were made for each composition. Both the tensile and compressive directions were parallel to extrusion direction (ED). Micro-hardness test was conducted at a load of 100 g with dwell time of 15 s. Microstructures and fractured surfaces were observed using a scanning electron microscope (SEM, TESCAN VEGA2) equipped with an energy dispersive X-ray spectrometer (EDS).

3. Results and discussion

3.1. X-ray diffraction pattern of GNP/Al composite

X-ray diffraction (XRD) analysis was carried out for pure aluminum and GNP/Al composite in a range of 2θ equal to 20–70° as shown in Fig. 2. It is clear from the figure that phases of pure aluminum are present at 2θ equal to 38.5°, 44.74° and 65.13°. Addition of GNPs leads to the formation of
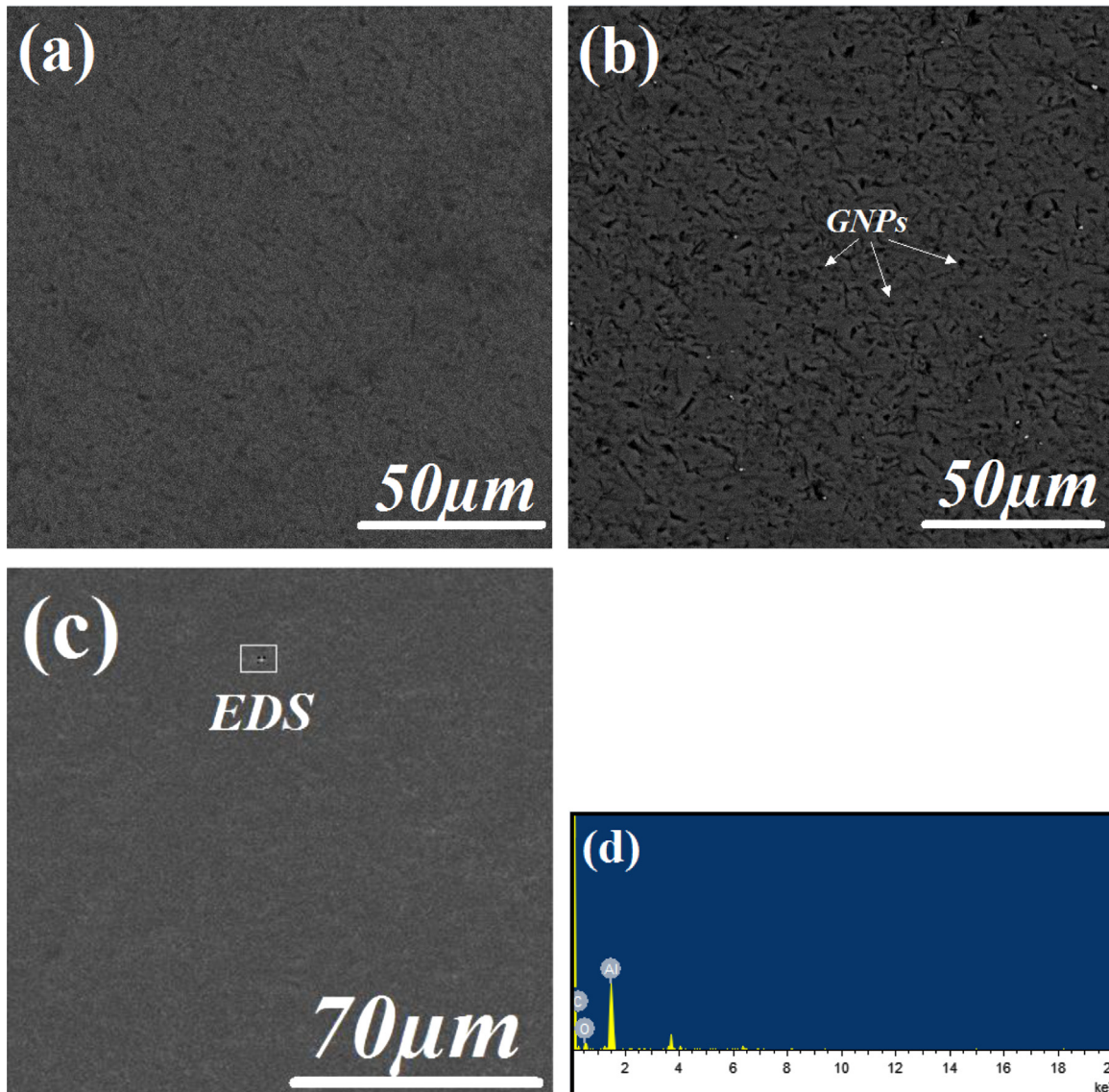

Fig. 3. SEM images of (a) pure aluminum; (b) Al/0.3 wt% GNPs composite; (c) Al/0.3 wt% GNPs composite with EDS; (d) EDS of selected area in (c).
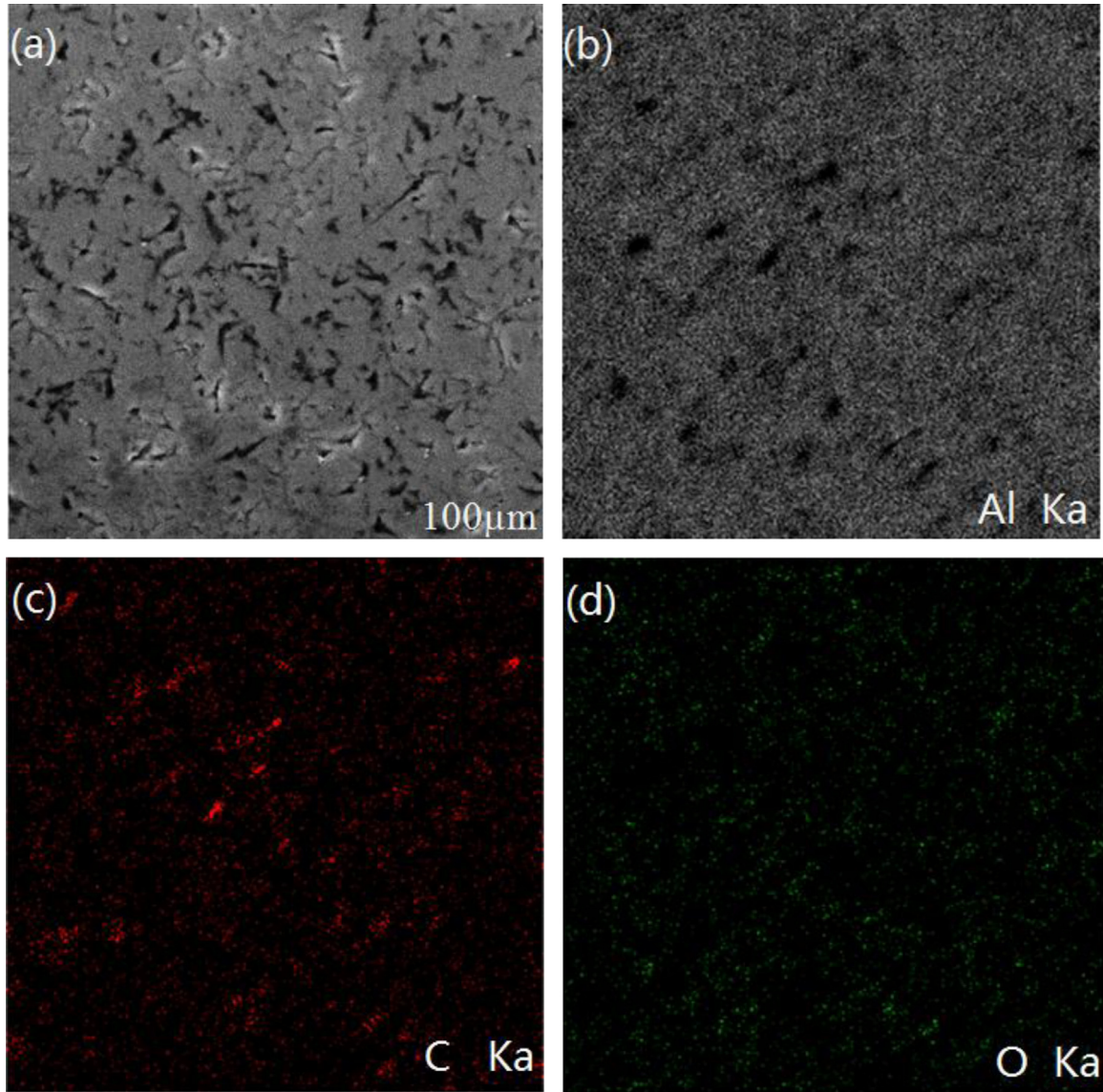
Fig. 4. X-ray mapping of (a) Al/0.3 wt% GNPs; (b) Al; (c) carbon; (d) oxygen.

Table 1
Theoretical and experimental densities of pure Al and Al/GNP composite.

Materials	Theoretical density (g/cm^3)	Condition	Measured density (g/cm^3)
Al	2.70	As-extruded	2.71
Al/0.3 wt% GNPs	2.69	As-extruded	2.70

Table 2
Room temperature mechanical properties of Al and Al–0.3 wt% GNP composite.

Materials	Tensile			Compression			Vickers hardness (HV)
	0.2%YS (MPa)	UTS (MPa)	δ (%)	0.2%YS (MPa)	UCS (MPa)	δ (%)	
Pure Al	170 ± 5	252 ± 4.5	13.4 ± 2	200 ± 4	493 ± 9	45.2 ± 4	76 ± 5
Al/0.3 wt%GNPs	195 ± 3	280 ± 5	9.53 ± 1.5	199 ± 3.4	457 ± 7.8	37.6 ± 3	85 ± 5

YS: yield stress; UTS: ultimate tensile strength; UCS: ultimate compression strength; δ: failure strain.

new peak at 2θ equal to $62.53°$ which confirms the presence of GNPs in the composite powder.

3.2. Microstructure of Al and GNP/Al composite

Scanning electron microscopy (SEM) was used to investigate the surface of pure Al and Al/GNPs composite. Fig. 3 shows the SEM images of (a) pure aluminum, (b) Al/0.3 wt% GNPs composite, (c) Al/0.3 wt% GNPs composite with EDS, and (d) EDS of selected area in (c). Microstructure of pure aluminum revealed good metallurgical bonding between the Al particles. Dark black regions are present due to oxidation during the sintering process. In Al/0.3 wt% GNPs composite small black wire like structures are GNPs which are uniformly distributed in the aluminum matrix. There is good chemical bonding between GNPs and aluminum particles. In order to investigate the adsorption of GNPs in the aluminum matrix, EDS analysis was performed. Fig. 3(c) and (d) shows the SEM images of Al/0.3 wt% GNPs composite and its corresponding point EDS analysis. EDS analysis shows the existence of a carbonaceous composition in the GNP/Al composites which confirms the presence of GNPs. Besides carbon there are small peaks of oxygen which reflects the small amount of oxidation during the sintering process.

Distribution of GNPs in the Al matrix was examined using the X-ray mapping. Fig. 4(a)–(d) shows the photomicrographs of Al/0.3 wt% GNPs composite with X-ray map. Fig. 4(c) shows that few Graphene Nanoplatelets are embedded into the Al matrix. These GNPs are beneficial to improve the mechanical properties of the composite.

3.3. Density and Vickers hardness analysis

Theoretical and experimental densities of pure aluminum and composite are listed in Table 1. It is clear from theoretical calculation that density of pure aluminum decreases with addition of GNPs. Measured experimental densities of both pure Al and composite are surprisingly higher than theoretical densities. This can be attributed to the formation of aluminum oxide (oxidation) during the sintering process. Since density of aluminum oxide is higher than aluminum and GNPs therefore, experimental densities are slightly higher than theoretical densities. Experimental density decreases with addition of Graphene Nanoplatelets. Since the density of GNPs is lower than density of pure Al, therefore composites exhibits lower density than pure aluminum. Also at high sintering temperature, diffusion of atoms is easier which leads to better sinterability of composite. The sintering process changes the dimensions of the composite due to shrinkage, which influences the density of composite.

The Vickers method was used to investigate the hardness of pure aluminum and it's composite. From Table 2 we can observe that hardness of composite is higher than that of pure aluminum. Increased hardness of composite can be attributed to uniform distribution of harder GNPs nanoparticles in the nano-composite, as shown in Fig. 4.

3.4. Tensile strength and fracture surfaces analysis

Mechanical strength of pure Al and Al/0.3 wt% GNPs composite is presented in Table 2 and Fig. 5. The addition of 0.3 wt% GNPs to pure Al leads to increase in yield strength and ultimate tensile strength (up to 195 and 280 MPa respectively) with 9.53 failure strain %. Increased strength can be attributed to the basic strengthening mechanism of the Al/0.3 wt% GNPs composite.

Graphene Nanoplatelets have coefficient of thermal expansion of $10^{-6}\,K^{-1}$ which is considered to be the same as graphite. On the other hand coefficient of thermal expansion of aluminum is $23.6 \times 10^{-6}\,K^{-1}$. Therefore Aluminum–Graphene Nanoplatelets composites have significant coefficient of thermal expansion mismatch which would result in prismatic punching of dislocations at the interface, leading to the strengthening of the composite matrix. Dislocation density depends on the surface area of reinforcement particles. Smaller the particles, higher the dislocation density which results in increased strength of composite [13]. Moreover, movement of dislocations in the pure aluminum is affected by GNPs particles which act as obstacles [14]. At high temperature diffusion rate is high which changes the mechanical properties
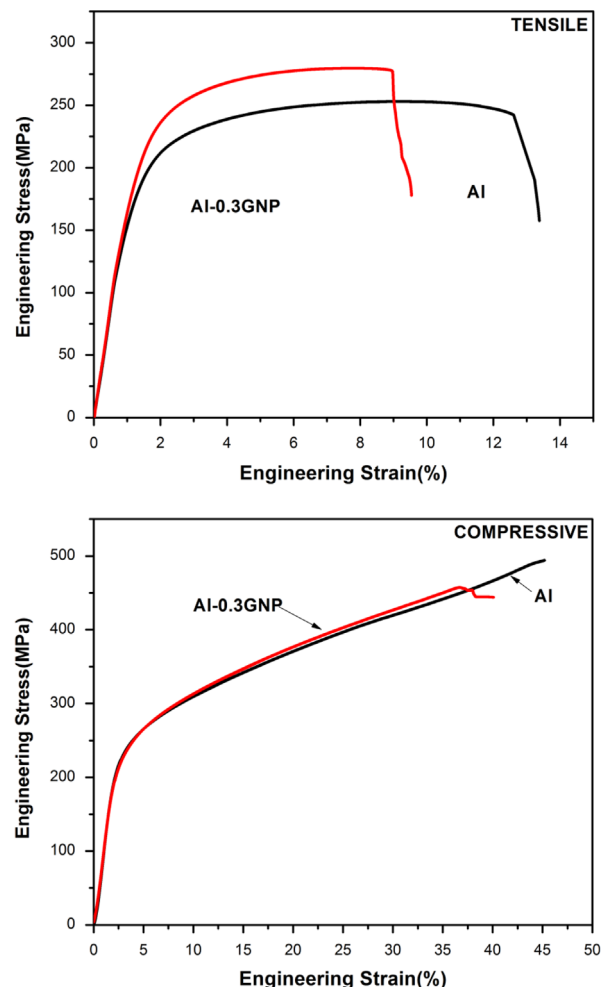

Fig. 5. Tensile and compression test of pure Al and Al/0.3 wt% GNPs composite.

of alloy but when reinforcement particles are added to the matrix then distance between them decreases. As a result, the dislocations face more obstacles during their motion leading to the dislocations pile up, therefore the strength of the composite increases. An increase in yield strength of the composites due to difference in CTE, $\Delta\sigma_{CTE}$ can be expressed by the following Eq. [15,16]:

$$\Delta\sigma_{CTE} = \alpha Gb\sqrt{12\Delta T\Delta Cf_v/bd_p} \qquad (1)$$

where $\Delta\sigma_{CTE}$ is change in yield strength due to CTE; α is a constant (its value is 1.25); G is the shear modulus of Al matrix; b is Burgers vector of matrix; ΔT is change in temperature; ΔC is difference in CTE between matrix and reinforcement (CTE for Al is $23.6 \times 10^{-6}\,K^{-1}$); f_v is volume fraction of reinforcement and d_p is mean particle size of reinforcement.

Orowan looping [17] also plays an important role in strengthening mechanism, which results due to the restricted movements of the dislocations caused by insertion of sub-micrometer to nanometer scales particles (GNPs nano-particles). Besides particle size, a uniform dispersion of reinforcing particles is also important in order to have as many particles as possible to take part in this strengthening mechanism [18]. Addition of GNPs nano-particles leads to formation of residual dislocation loops around each particle (after a dislocation bows out and by passes it) which produces a back stress that prevents dislocation's migration leading to an increase in the yield stress. The increase in yield strength of the composites due to Orowan looping, $\Delta\sigma_{Orowan}$ can be expressed using following equation [19]:

$$\Delta\sigma_{Orowan} = \frac{0.13Gb}{d_p[(1/2f_v)^{1/3}-1]} \ln\left(\frac{d_p}{2b}\right) \qquad (2)$$

Load transfer from matrix to reinforcement can be explained using Shear lag model [20]. Load transfer from matrix to reinforcement depends largely on interfacial bonding between the matrix and the reinforcement by interfacial shear stress. Fig. 4 shows that GNPs are uniformly embedded in the Al matrix leading to efficient load transfer form matrix to reinforcement and result in an increased strength of composite. Increase in yield strength of composites due to load transfer, $\Delta\sigma_{LT}$ can be estimated using following equation [15, 21]:

$$\Delta\sigma_{LT} = \frac{f_v\sigma_m}{2} \qquad (3)$$

where σ_m is the yield strength of the matrix.

The tensile strength of Al/0.3 wt% GNPs composite was measured to be 280 MPs whereas for unreinforced Al matrix, tensile strength was observed to be 252 MPa. Just 11.1% improvement in tensile strength was achieved by the addition of GNPs reinforcement particles. One possible reason for low tensile strength may be that the used GNPs are few layer graphene and their fracture strength is much lower as compared to the single layer graphene sheets (125 GPa). Second possible reason may be due to existence of pores
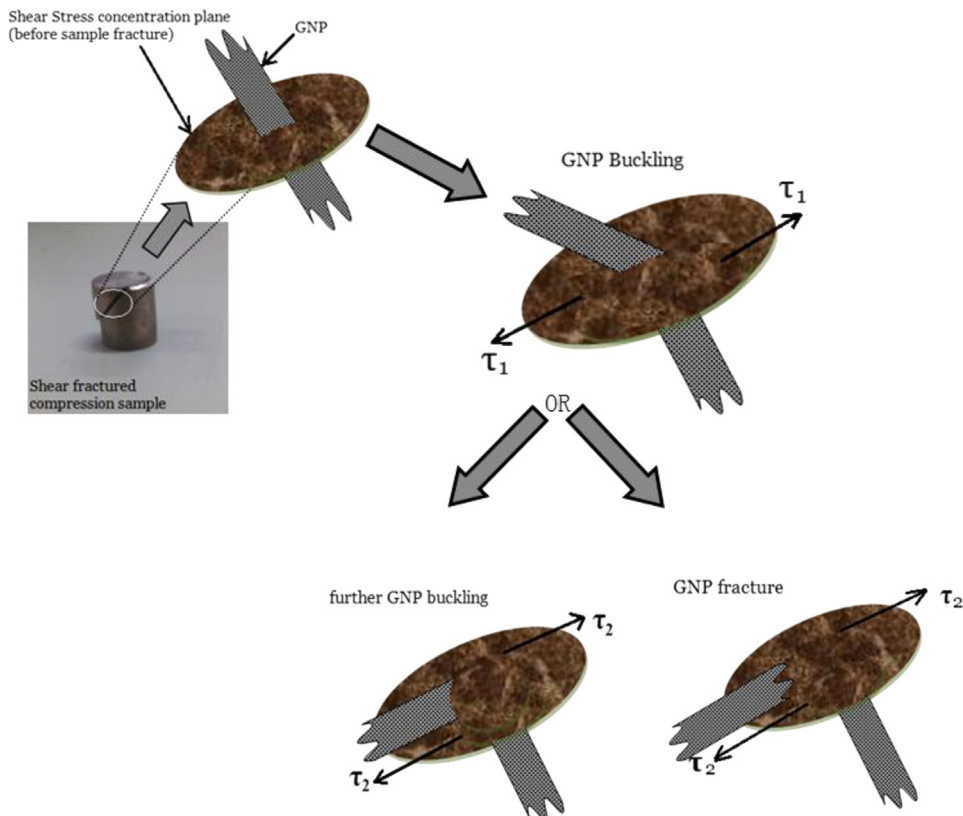

Fig. 6. Schematic diagram illustrating compressive shear buckling of GNP in Al–0.3 wt% GNP nano-composite (τ_1 and τ_2 are planar shear stresses where $\tau_1 < \tau_2$).

and cavities which were left during cold pressing, therefore these pores are responsible for cracks initiation during fracture (Fig. 7). Third and most evident reason is that most of the GNPs were not aligned along the tensile direction (out of plane), and out-of-plane strength (i.e. weak physical bonding between atoms of adjacent layers) of graphene is much less than in-plane strength (i.e. strong chemical bonding between adjacent atoms in same layer). This phenomenon is confirmed by Fig. 7(c) where GNPs are multilayer. It can be observed that the GNPs are perpendicular to the tensile direction; therefore these GNPs are responsible for low strength and ductility of composite. Furthermore, there is vast difference in melting point and compressive strength of the constituents. Therefore, GNPs particles act as a barrier for diffusion and rearrangement of particles which results in high porosity in the composite. Increasing particle size of GNPs increases the porosity; however sintering temperature lowers the porosity [22]. In conclusion, high temperature results in denser structure

and low porosity of the composite. The dependence of diffusion coefficient on sintering temperature [23] is explained by the following equation:

$$D = D_O \exp(-Q/RT) \tag{4}$$

where D is the diffusion coefficient, D_O (2×10^{-5} ms^{-1}) is diffusion constant, Q (22,500 J mol^{-1}) is activation energy, R is Boltzmann's constant and T is the sintering temperature. Using the value of sintering temperature, diffusion coefficient can be calculated. Denser structure is obtained at high temperature with low porosity.

Compressive strength of Al–0.3 wt% GNPs composite is surprisingly lower than pure Al. 0.2% CYS of pure Al and Al–0.3 wt% GNP composite is same. But Al–0.3 wt% GNPs composite shows ultimately compressive strength and failure strain (%) lower than pure Al. Lower compressive strength of Al–0.3 wt% GNPs composite can be attributed to following reasons. Tensile strength of graphene is high due to its 2 dimensional
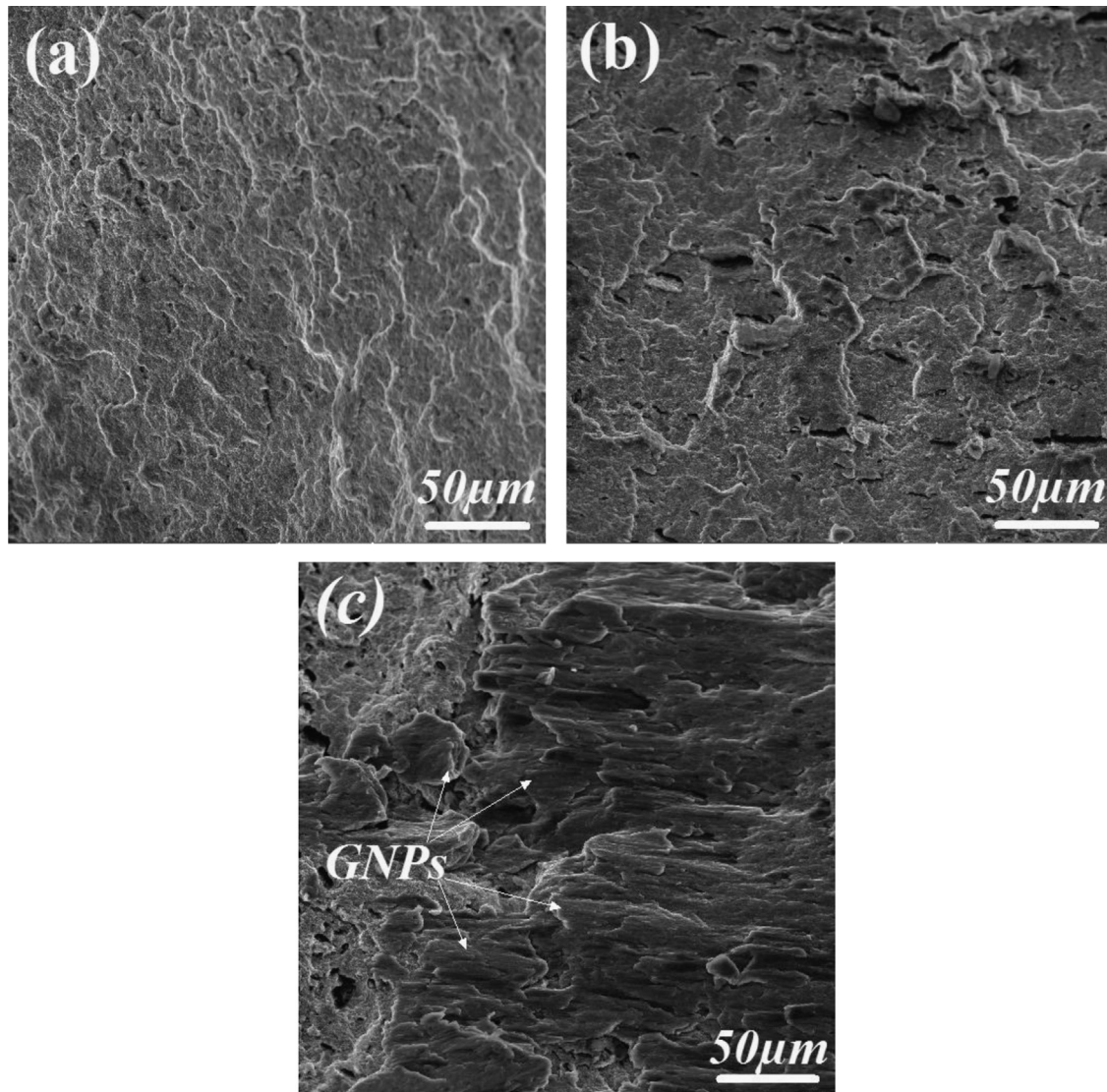

Fig. 7. SEM fracture surfaces of (a) pure aluminum; (b) Al/0.3 wt% GNPs; (c) Al/0.3 wt% GNPs at region with GNPs perpendicular to the extrusion direction [tensile].

structure. But under compression test, graphene is soft due to flake buckling, therefore it cannot be squeezed. Also under tensile graphene flakes strains more than under compression test [24]. If Graphene Nanoplatelets are parallel to the extrusion direction, then after compressive load is applied, graphene flakes buckles and bent at an angle of 45° (Fig. 6). Further increasing compressive load graphene inclined at an angle of 45° again buckles or breakup leading to decrease in compressive strength of the composite (Fig. 6). If Graphene Nanoplatelets are perpendicular to extrusion direction then they don't contribute to the compressive strength. If graphene is multilayer then bonding between 2 adjacent layers of graphene is wonder Waals force. These forces are very week. Therefore when compressive strength is applied there is slipping between graphene layers (graphene–Al bonding is strong than wander Waals forces). These are possible factors which are responsible for low compressive strength of Al–0.3 wt% GNP nano-composite.

Tensile fracture behavior of both monolithic material and composite material is shown in Fig. 7. It is clear from the SEM fracture images that the dark pores and cavities were left during compacting and some of them were produced during the sintering of the green billets. These pores and cavities are responsible for the crack and fracture initiation [25–27]. There are few small pores in pure aluminum so the material is not so easy to be fractured. However, fracture surface of Al/0.3 wt% GNPs composite (Fig. 7(b)) exhibits a lot of small cavities where GNPs were parallel to extrusion direction and pulled out during tensile loading. The reason is poor bonding between GNPs and Al particles.

4. Conclusions

The aluminum–graphene nanoplatelets composite has been successfully synthesized through semi-powder metallurgy method followed by a hot extrusion technique. Compared to pure Al, synthesized composite exhibited higher hardness and tensile strength which might be attributed to the geometry necessary dislocation generation (due to mismatch in CTE between matrix and reinforcement), Orowan looping and efficient load transfer from soft matrix to the strong reinforcement. Surprisingly the ultimate compressive strength of the composite was lower than pure aluminum which may be due to the flake buckling nature of two dimensional flexible graphene sheets. Furthermore, the proposed semi-powder method is free of ball milling and has great potential to fabricate the metal composites reinforced with nano-materials.

References

[1] A.K. Geim, K.S. Novoselov, Nat. Mater. 6 (2007) 183–191.
[2] C. Lee, X.D. Wei, J.W. Kysar, J. Hone, Science 321 (2008) 385–388.
[3] A.A. Balandin, S. Ghosh, W. Bao, I. Calizo, D. Teweldebrhan, F. Miao, et al., Nano Lett. 8 (3) (2008) 902–907.
[4] K.I. Bolotin, K.J. Sikes, Z. Jiang, M. Klima, G. Fudenberg, J. Hone, et al., Solid State Commun. 146 (9) (2008) 351–355.
[5] V. Goyal, A.A. Balandin, Appl. Phy. Lett. 100 (2012) 073113.
[6] K.M.F. Shahil, A.A. Balandin, Nano Lett. 12 (2012) 861–867.
[7] K.M.F. Shahil, A.A. Balandin, Solid State Commun. 152 (2012) 1331–1340.
[8] E.S.M. Sherif, A.A. Almajid, F.H. Latif, H. Junaedi, Int. J. Electrochem. Sci. 6 (2011) 1085–1099.
[9] W.R. Oso′rio, N. Cheung, L.C. Peixoto, A. Garcia, Int. J. Electrochem. Sci. 4 (2009) 820–831.
[10] X. Lei, J. Ma, Y. Sun, Int. J. Electrochem. Sci. 6 (2011) 537–580.
[11] S.R. Bakshi, D. Lahiri, A. Agarwal, Int. Mater. Rev. 55 (1) (2010) 41–64.
[12] J Wang, Z. Li, G. Fan, H. Pan, et al., Scr. Mater. 66 (2012) 594–597.
[13] R.J. Arsenault, N. Shi, Mater. Sci. Eng. C (1986) 175–18781 (1986) 175–187.
[14] G.E. Dieter, Mechanical Metallurgy, third ed, McGraw-Hill, New York, 1976.
[15] J.W. Luster, M. Thumann, R. Baumann, Mater. Sci. Technol. 9 (1993) 853–862.
[16] W.S. Miller, F.J. Humphreys, Scr. Metall. Mater. 25 (1991) 33–38.
[17] E.Z. Orowan, Nucl. Phy. 89 (9–10) (1934) 634–659.
[18] R.M. German, Powder metallurgy science, Princeton, NJ, Metal Powder Industries Federation, USA, 1994.
[19] Z. Zhang, D.L. Chen, Scr. Mater. 54 (2006) 1321–1326.
[20] T.W. Clyne, An Introduction to Metal Matrix Composites, Cambridge University Press, Cambridge, UK, 1995, p. 26–43.
[21] R.M. Aikin Jr, L. Christodoulou, Scr. Metall. Mater. 25 (1991) 9–14.
[22] K.H. Min, S.P. Kang, D.K. Kim, Y.D.J. Kim, J. Alloys Compd. 400 (1–2) (2005) 150–153.
[23] D.A. Porter, K.E. Easterling, Phase Transformations in Metals and Alloys, Second Edition, McGraw-Hill, New York, 1980.
[24] G. Tsoukleri, J. Parthenios, K. Papagelis, R. Jalil, A.C. Ferrari, A.K. Geim, K.S. Novoselov, C. Galiotis, Small 5 (21) (2009) 2397–2402.
[25] M. Rashad, F.S. Pan, A. Tang, M. Asif, J. She, J. Gou, J.J. Mao, H.H. Hu, J. Compos. Mater. (2014) http://dx.doi.org/10.1177/0021998313518360, in press.
[26] M. Rashad, F.S. Pan, M. Asif, A. Tang, J. Ind. Eng. Chem. (2014) http://dx.doi.org/10.1016/j.jiec.2014.01.028, in press.
[27] M. Rashad, F.S. Pan, A. Tang, Y. Lu, M. Asif, S. Hussain, J. She, J. Gou, J.J. Mao, J. Magn. Alloys 1 (2013) 242–248.